ELSEVIER

Thermochimica Acta 355 (2000) 59–68

thermochimica acta

www.elsevier.com/locate/tca

Thermal analysis: the next two decades

Stephen Z.D. Cheng*, Christopher Y. Li, Bret H. Calhoun, Lei Zhu, William W. Zhou

Maurice Morton Institute and Department of Polymer Science, The University of Akron, Akron, OH 44325-3909, USA

Received 18 August 1999; accepted 14 September 1999

Abstract

As some of the most important analytical methods, thermal analysis techniques have been greatly improved and perfected due to the requirements of materials characterization. Over the past four decades, the major developments have been associated with computerizing thermal analysis techniques. In the coming 20 years, thermal analysis techniques will continue to develop in at least two different directions. First, more precise measurements can be carried out using traditional thermal analysis techniques by making a small extra effort. This will lead to a variety of new information regarding a material's structure interface and morphology obtained from the results. Second, thermal analysis techniques can be combined with other in-situ temperature-controlled experiments, such as diffraction, scattering, microscopy, and spectroscopy, for investigation of the structure and dynamics of materials. This will generate information of the structural evolution with changing thermal properties and therefore, greatly aid in the understanding of structure–property relationships of the materials.

Keywords: Thermal analysis; Structure–property relationship; Polymers

1. Introduction

The term thermal analysis is applied to any technique which involves a measurement of a material's specific property while the temperature is controlled (either changed or maintained) and monitored. If one looks back upon the history of thermal analysis, the principle was not completely understood until the macroscopic properties of heat and temperature were correctly placed, and the microscopic origin of these properties, namely, molecular motion, was recognized. It is not surprising, then, that thermal analysis techniques started to obtain significant attention only after the field of classical thermodynamics was established, and achieved a rapid development along with the growth of materials science.

The basis of thermal analysis includes macroscopic theories of matter, which consist of equilibrium and irreversible thermodynamics and kinetics. The kinetics aspect provides a link to the microscopic description via molecular models. The macroscopic parameters in thermodynamics include temperature (T), pressure (P), enthalpy (H), entropy (S), Gibbs energy (G) and other macroscopic variables, as well as material parameters that may be used to describe a

* Corresponding author. Tel.: +1-330-972-6931; fax: +1-330-972-8626.
E-mail address: cheng@polymer.uakron.edu (S.Z.D. Cheng)

0040-6031/00/$ – see front matter
PII: S0040-6031(00)00437-8

system. The basis for this kind of description comes from three empirical laws of classical thermodynamics, such as the conservation of energy, etc. However, the microscopic parameters deal with atomic and/or molecular symmetry and dynamics. The structural symmetry, including translation, rotation, and reflection is described by the Euclidean group. Since a fluid (liquid or gas) is invariant under all of these operations, its symmetry group is the Euclidean group. Fluids have the highest possible symmetry, and thus, they have the largest number of symmetry operations. This implies that fluids have short-range order but no long-range order. Liquids and gases, therefore, cannot be distinguished by symmetry. This is reflected in the fact that one may move continuously from a liquid to a gas phase simply by going around a critical point. All other equilibrium phases of matter are invariant only under certain subgroups of the Euclidean group, and therefore, have lower symmetry than fluid phases. This reduced symmetry is the cause of the ordered structures that are introduced in other phases. On the other hand, mechanics can be used to express atomic or molecular motions and interactions by providing a series of differential equations. However, this method can only solve problems considering motion and interactions among a few bodies. For a system that contains a large number of atoms or molecules, a mechanics approach does not yield analytical results. To establish a relationship between the macroscopic and microscopic descriptions, one has to understand that the macroscopic thermodynamic description of a system is an average of the microscopic mechanical motions and interactions of the atoms or molecules. As a result, statistical mechanics serves as a bridge that connects these two descriptions [1–3].

The traditional thermal analysis techniques include thermometry, calorimetry, differential thermal analysis (DTA), thermomechanical analysis (TMA), and thermogravimetric analysis (TGA). In recent years, dynamic mechanical and dielectric analyses (DMA and DEA) have also been included among thermal analysis techniques. Besides thermometry, which provides the standard of temperature measurements, the general scheme of these thermal analysis techniques is to measure macroscopic responses of materials with respect to the temperature change. For example, calorimetry represents the effort to measure heat in any of its manifestations. DTA is for the measurement of temperature change. TMA is designed for the measurement of dimensional changes. TGA measures weight changes. DMA and DEA are for the materials' responses towards external alternating force and electric fields with changes in temperature, respectively. Generally speaking, thermal analysis techniques provide accurate information regarding macroscopic property changes with temperature; however, structural information cannot be obtained by these techniques which precisely explains the reasons for these macroscopic property changes. Therefore, for many years, thermal analysis techniques have been viewed as a part of the property characterizations of materials in establishing structure–property relationships in materials science. Detailed information regarding this area can be obtained from a number of excellent reviews and books cited in [4–11].

As we are standing at the gate preparing to enter the next century, it is difficult to provide a vision of thermal analysis for the next two decades if we look back upon the past 20 years at how much progress and development has been made in this area. However, it is our point of view that thermal analysis techniques, as an important part of materials characterization, will continue to grow and make progress in at least two specific areas. They are: (1) more precise and meaningful measurements in these techniques; and (2) new developments in obtaining the temperature dependence of a material's structure and dynamics.

Regarding the first area of further development of thermal analysis techniques, it is important to correct an often-misunderstood view held by many materials researchers. Namely, thermal analysis techniques are simple and quick. Therefore, less attention has been paid to how to be precise in carrying out the measurements using these techniques, how to extract the most information from experimental data, and how to correctly explain the experimental results obtained. In fact, a relatively small effort to do better thermal analysis experiments may lead to substantial advances in understanding a material's structure and property relationships.

When we introduce temperature-controlled experiments into structural and molecular dynamic characterizations, which is the second area of making progress in the next two decades it is possible to extend thermal analysis techniques to a variety of

experimental research fields. Over the past two decades, temperature and time-dependent experiments in the determination of structures and dynamics have been quickly developed. These in-situ experiments can provide instant observations of structural and dynamic changes during phase transformations. Furthermore, new temperature-controlled techniques have gradually appeared which measure phase behaviors of materials in small dimensions, such as in thin films and surfaces, with substantially high resolutions. These developments are not only in the areas of the reciprocal spaces (such as scatterings) but also in the real spaces (such as microcopies).

2. More precise measurements in traditional thermal analysis techniques

The revolution of the computer data treatment process leads to a number of new opportunities to obtain more precise measurements in traditional thermal analysis techniques. However, most of the thermal analysis techniques to this point have been used solely to obtain phase transition information. For example, in DSC and DTA measurements, the widest application is to report the transition behavior such as melting point, crystallization temperature and glass transition temperature. Heats of first-order transitions are often studied although the base line selected for integration of the peak area is still an obscure factor. For TMA experiments, a common observation is the temperature where a sudden change of the sample dimensions is recorded. This usually corresponds to the transition behaviors. Needless to say, DMA and DEA measurements are also focused on the relaxation peak temperatures and are frequency dependent. In fact, by simply using a small amount of extra effort in these thermal analysis techniques, experimental data consisting of the absolute values of a material's properties and additional structural and morphological information can be obtained.

This is particularly true in polymer materials. Polymers are a rich field for examples of phases and phase transformations. Due to the long chain nature, the microscopic dynamics in polymers are in multiple size domains. Their phase behaviors are usually described using the concept of metastable states, not only the classical one but also the metastable states in other structural hierarchies [1–3]. In many cases, the classical metastable states may be interwoven with other metastable states to cause complicated experimental observations. For example, when liquid–liquid phase separation occurs in solutions or blends, the system does not proceed to a state of ultimate stability, such as in a phase-separated mixture of water and oil, but rather the mixture provides a variety of microscopic phase morphologies. The formation mechanisms of these phase morphologies are determined by nucleation or by spinodal decomposition. If the phase separated polymer blends always quickly reached their ultimate stable states, these metastable phase morphologies would disappear and this research field might not be as interesting and rewarding as it is today. A more complicated case is where one of the components is crystallizable after the phase separation. An additional crystal morphology may form within one of the phase morphologies formed by the liquid–liquid phase separation. On the other hand, when a vitrification is introduced into a system that has undergone the liquid–liquid phase separation, this process may interrupt the phase separation and thus the phase morphology may be 'locked in'. This can happen in either liquid–liquid phase separation or crystallization, and the microscopic phase and/or crystal morphologies may be frozen. Therefore, there are several hierarchies of morphologies, each with a corresponding hierarchy of metastabilities.

For the crystalline state in chemically uniform thermoplastic homopolymers, a fully crystalline state with extended chain crystals has never been reached. In reality, attempts at this have been shown to possess an amorphous-crystalline ratio which is always less than 100% (crystallinity<100%, therefore, they are semicrystalline materials) [12–18]. The reasons preventing complete crystallization from occurring come from a range of factors all of which are associated with the long chain nature of the macromolecules, and are kinetic in origin. However, the amorphous content in these semicrystalline polymers is composed of a range of states from localized fully amorphous domains to the surface regions of the crystals, with intermediate stages which may be characterized as strained amorphous and rigid amorphous.

Examining a few examples of metastable states given here, we quickly realize that we lack a unified definition to quantitatively formulate these states.

However, one distinct and definitive structural feature, the chain folded lamellar crystal, may provide an opportunity to precisely illustrate the concept of a morphological metastable state, which is a type of circumstantial metastable state. This is not only uniquely important for the case of crystalline polymers, but also essential to reach wide generalizations in the phase behavior of matter in order to discuss size-induced metastabilty. The concept of a morphological metastable state is based on the fact that the basic crystal habit in a flexible chain polymer is lamellae containing chain folded conformations. The thickness of lamellar crystals (l) is equal or related to the fold length and generally in the range of 10–50 nm. The melting (or dissolution) temperature of the crystals represents the thermodynamic stability of the lamellar crystals. This can be expressed quantitatively through the Gibbs–Thomson relation which, as applied to polymer crystals in the Hoffman–Weeks formulation [19], is

$$T_m = T_m^0\left(1 - \frac{2\sigma_e}{l\Delta H}\right) \quad (1)$$

where T_m is the melting temperature of the crystal having a thickness l, T_m^0 is the ultimate equilibrium crystal melting temperature (i.e., with $l \to \infty$), ΔH is the heat of fusion of crystal melting and σ_e is the surface free energy of the basal, or fold containing plane of the lamella (although a similar equation can be easily derived when the lateral side surface energy is taken into account, the effect of the lateral side surface to the crystal stability is generally considered negligible). In almost every semicrystalline polymer with a lamellar crystal habit, Eq. (1) is closely obeyed.

The reason for the correlation of the lamellar thickness to ΔT indicated in Eq. (1) lies in kinetics. Based on classical nucleation theory, at a particular ΔT only one lamellar thickness is favored; the so-called kinetically optimized thickness. This is because that at each ΔT there is only one nucleation barrier set at the bottom of a hyperbolic paraboloid free energy (F) surface with respect to the nucleus size (the lowest F barrier). Generally, after primary nucleation, growth along the thickness direction in polymer lamellar crystals is found to be negligible. Hence, thickness could be regarded as a distinct metastable structure, or a morphological 'polymorph' and consequently be called a 'morphological metastability'. Therefore, the morphological metastability caused by lamellar thickness can be considered the first level in the hierarchies of circumstantial metastability [1–3].

On the other hand, the glass transition is a kinetic process, which is largely dependent upon time of measurements. Since the structural symmetry does not change above and below the glass transition temperature (T_g) but the molecular motion differs, at fixed heating and cooling rates, the glass transition process looks like a thermodynamically second-order transition such as a sudden change in heat capacity, coefficient of thermal expansion, or compressibility. However, when the cooling rate and heating rate are not identical, or annealing at a temperature near but below the T_g, enthalpy and volume relaxation can be clearly observed. Furthermore, these relaxation processes have been found to not exactly be parallel from one to another. Instead, one process can take place before the other. All of these relaxation processes, however, have always been shown to possess multiple frequencies rather than a single frequency relaxation, such as with an Arrhenius process. In semicrystalline polymers, the glass transition process is always associated with the amorphous part of the materials, which become mobile above the T_g.

Therefore, thermal analysis techniques should be powerful tools to characterize the properties in identifying these metastable states to understand the effects of phase size, dimensionality and composition on the materials properties. One well-known example is the characterization of the interfacial structures in semicrystalline polymers: identifying so-called rigid amorphous fractions using DSC and/or DMA/DEA methods. This concept can be traced back as far as 30 years ago. However, extensive study has been carried out in the past 10–15 year [20–27]. It is known that the crystallinity concept invokes the two-phase model, which simply divides the system into a perfectly ordered crystalline region and an amorphous region with sharp boundaries. In order to examine the validity of this two-phase (crystallinity) model using DSC, one needs prior established heat capacity data in solid and liquid states of the polymers. With this data, one could, therefore, predict that for a semicrystalline polymer

$$w^c = 1 - \frac{\Delta c_p\ (\mathrm{m})}{\Delta c_p\ (\mathrm{a})} \quad (2)$$

where w^c is the weight-fraction crystallinity and is usually obtained by DSC measurements, density determination and/or wide angle X-ray diffraction experiments. The terms Δc_p (m) and Δc_p (a) are the heat capacity increases at T_g for the semicrystalline sample and the amorphous sample, respectively. Surprisingly, a wide variety of behaviors that deviates from the ideal two-phase model exist. A positive heat capacity deviation is observed for practically all polymers long before the clearly recognized fusion endotherm begins. This has been linked to pre-melting and/or defect formation. For PB and polytetrafluoroethylene (PTFE) these positive deviations close to the melting temperatures are well-analyzed [4,28]. The heat capacities of polyoxymethylene (POM) show, on the other hand, a negative deviation at somewhat lower temperatures relative to the melting temperature [20,21]. This reveals an extra fraction in the polymer which contributes neither to the glass transition at T_g nor to the heat of fusion at T_m. This fraction has been called the 'rigid amorphous fraction'. In POM this rigid amorphous fraction does not show any signs of softening up to its melting. Similar measurements in i-PP exhibit a rigid amorphous fraction that is gradually unfreezing which leads to the occasionally observed 'doub1e glass transition' [29]. As a result, if a rigid amorphous fraction exists in a semicrystalline polymer, the two-phase model cannot be used to describe that system, and

$$w^c < 1 - \frac{\Delta c_p \ (\mathrm{m})}{\Delta c_p \ (\mathrm{a})} = f_r \tag{3}$$

The resulting difference Eqs. (2) and (3) is the rigid amorphous fraction in a polymer, $f_r - w^c$. Most of the thermoplastic engineering polymers such as PEEK [22], PPS [23], PPO [24], PET [30], PBT [25], PEN [26] and polyimides [27], show this kind of behavior which is critically dependent upon the thermal history of the samples. Fig. 1 shows three fractions in a high molecular weight linear PPS sample, in which the non-mobile amorphous fraction above the T_g represents the rigid amorphous fraction. More complicated situations may also be observed by combining both positive and negative deviations of heat capacities in a semicrystalline polymer. Other structural characterization methods are necessary to distinguish these deviations and to separate both effects.

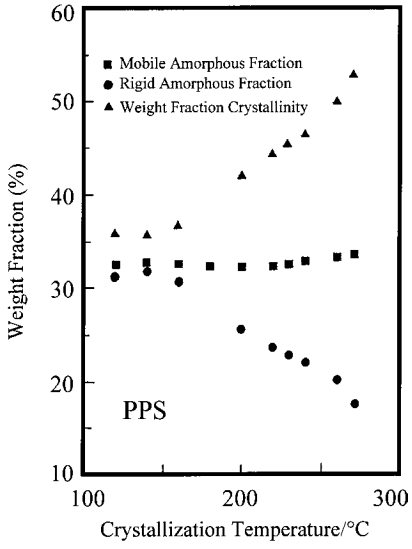

Fig. 1. Three fractions of PPS crystallized at different temperatures.

3. In-situ temperature-controlled experiments in structures and dynamics

During the past two decades, materials' structures and dynamic properties have been extensively investigated under in-situ temperature controlled fashion. This is partially due to the development of stronger sources and more sensitive detectors in diffraction, scattering, microscopic and spectroscopic experiments. Since traditional thermal analysis techniques only provide information of thermal events, any structural and dynamic behavior changes that are detected in these techniques cannot be directly identified. A combination of structural and dynamic characterizations with thermal analysis techniques is thus attractive to materials researchers. The most noticeable efforts have been in-situ temperature-controlled synchrotron wide angle X-ray diffraction (WAXD) and small-angle X-ray scattering (SAXS), temperature-controlled solid state carbon-13 nuclear magnetic resonance (NMR), and temperature-controlled atomic force microscopy (AFM) experiments. The development of various types of dynamic DSC can also be viewed as combined techniques of DSC and alternating heating schemes.

One example is the crystallization of low molecular weight (LMW) poly(ethylene oxide) (PEO) fractions

from the melt. In the 1960s it was recognized that LMW PEO which had a low degree of polydispersity and chain lengths within a desired range displays at least the main features of truly monodisperse materials. The most notable feature that is observed in PEO having MWs ranging from 2000 to 10 000 is that of integral chain folding (IF). Accordingly, the lamellar thickness, hence fold length, is not a continuous function of ΔT, such as with usual high MW polymers, but varied stepwise. Specifically, lamellar thickness decreases with increasing ΔT and on subsequent heat annealing, increases with annealing T, where the steps corresponded to the extended, once-folded, twice-folded, etc., chain lengths. These results were first obtained by SAXS experiment [31–33] and subsequently by PLM and transmission electron microscopy (TEM). [33–38]. The latter two results further displayed some remarkable effects relating to morphology, crystal growth and crystal stability. We ask whether the chain molecules are organizationally associated with each other, forming an IF chain conformation during crystallization, or whether they are 'blind' to the presence of other chains until their neighboring segments have crystallized. In the former case, the IF crystal forms directly from the melt. Otherwise, a non-integral folding chain NIF crystal appears as an initial transient state.

Although DSC results show that there are a few exothermic processes overlapped during isothermal crystallization, the correspondence of these exothermic processes with the formations of different types of crystals has not been known until recently. The in-situ temperature-controlled synchrotron SAXS experiments find that in the course of crystal evolution the IF crystal state was preceded by formation of crystals having intermediate thickness between those for the discrete IF crystal values. Therefore, these correspond to the NIF crystals. The nearest IF thickness is finally attained through isothermal thickening or rather remarkably, thinning in isothermally conducted experiments [39–49]. Therefore, the exothermic processes found in isothermal DSC observations can be precisely assigned to formations of the NIF and IF crystals.

Furthermore, over a wide range of undercooling, NIF crystals formed initially, and then were transformed into IF crystals. Although the NIF crystal is thermodynamically less stable, kinetically it grows faster [1,2,39–49]. Compared to the IF crystals, the NIF crystals are morphologically metastable. Fig. 2 shows the formation of NIL crystals in a PEO fraction with MW=3000 crystallized at 43°C as an example. It is clear that the NIF crystal having a fold length of about 13.6 nm appears first, which is in between the fold lengths of extended chain crystals [IF (n=0)] (19.3 nm) and once-folded crystals [IF (n=1)] (10.0 nm). The fold length of the NIF crystals is found to be crystallization T dependent, similar to the observed changes of fold length in polymer crystals. It is interesting to find that both thickening [NIF→IF (n=0) crystals] and thinning [NIF→IF (n=1) crystals] processes occur at constant T_es during the NIF→IF crystal transformation. More importantly, these processes continue to occur long after the overall crystallization reaches completion. The existence of the NIF crystals as well as these isothermal transformations have also been independently proven by Raman longitudinal acoustic mode experiments [50,51].

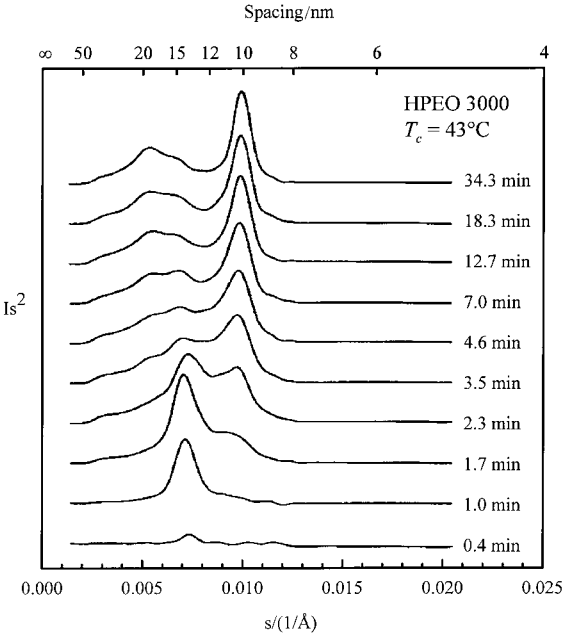

Fig. 2. Set of in-situ temperature-controlled SAXS curves for a PEO (MW=3000) fraction crystallized isothermally at 43°C for various times.

It is known that the size of crystals (such as lamellar fold length) is critically associated with the crystal thermodynamic stability, and may obey the Thomson–Gibbs equation (or the Hoffman-Weeks equation in

polymer crystals). As a result, the thickening process is thermodynamically justified since the crystals are annealed into a more stable form. However, the thinning process in LMW PEO fractions is an issue which needs to be further discussed, similar to the case of the n-a1kanes [52,53]. When we think of thermodynamic and morphological criteria for these processes, one expects that if the Gibbs (free) energies of these crystals follow G(NIF)>G(IF, $n=i+1$)>G(IF, $n=i$) and their fold lengths are L(IF, $n=i$)>L(IF)>L(IF, $n=i+1$), both thickening and thinning can take place [in the case of $i=0$ it implies that there are IF ($n=0$) and IF ($n=1$) crystals]. On the other hand, if G(IF, $n=i+1$)>G(NIF)>G(IF, $n=i$) and their fold lengths are L(IF, $n=i$)>L(NIF)>L(IF, $n=i+1$), this returns to the common case of polymer lamellar crystals in which the thinning process is forbidden. The explanation of the highest Gibbs F for NIF crystals is due to the inclusion of chain end defects within the Qc crystals and the rough fold surfaces. Both factors destabilize the crystals and increase the Gibbs F of the system. Therefore, the NIF crystal is the least stable crystal among these three states even though it possesses a fold length which is thicker than that of an IF ($n=i+1$) crystal. As a result, it can be rationalized that the F barrier to the formation of the NIF crystals must be the lowest among these three crystals and therefore, the LMW PEO molecules are trapped in this metastable state after the molecules overcome the NIF F barrier. Two F pathways exist for the NIF crystals to relax towards lower F states: one is the IF ($n=1$) crystal and another is the IF ($n=0$) crystal. The latter is the ultimate stable state among these three crystals. Furthermore, NIF crystals can also been found in the cases in which the fold numbers exceed on the transformation of the NIF→IF crystals thus explores relationships between two categories of metastability (classical versus morphological).

Another example is the molecular dynamics in different polymer liquid crystalline states detected using a combined techniques of DSC, in situ temperature-controlled WAXD and solid state C-13 NMR techniques. Liquid crystalline polymers have grown rapidly both in academia and industry during the last two decades. Like crystals, liquid crystal structures can also be identified by X-ray diffraction techniques. To this point, more than thirty phases have been identified based on different orders and symmetries in these phases [54,55]. All the phases exhibit their own thermodynamic properties which can be measured using DSC (heats of transitions and transition temperatures). They also possess diffraction characteristics identified by WAXD techniques (the phases are defined by positional, bond orientational and molecular orientational order) and molecules in each state have different dynamics detectable by NMR experiments. For instance, a series of liquid crystalline polymers synthesized from 1-(4-hydroxy-4′-biphenyl)-2-(4-hydroxyphenyl) propane and 1,15-dibromopentadecane show several highly ordered smectic phases and smectic crystal [56–62]. Although the DSC diagram shown in Fig. 3 does not provide information regarding the phase structures, in-situ temperature-controlled WAXD experiments identify these structures, also shown in Fig. 3. Therefore, this polymer possesses multiple liquid crystalline states and its transition sequence can be written as [57].

$$\mathrm{I} \underset{18.14\ \mathrm{kJ/mol}}{\overset{150^{\circ}\mathrm{C}}{\leftrightarrow}} \mathrm{S_F} \underset{6.21\ \mathrm{kJ/mol}}{\overset{130^{\circ}\mathrm{C}}{\leftrightarrow}} \mathrm{SC_G} \underset{13.69\ \mathrm{kJ/mol}}{\overset{118^{\circ}\mathrm{C}}{\leftrightarrow}} \mathrm{SC_H} \overset{23^{\circ}\mathrm{C}}{\leftrightarrow} T_g$$

Beginning at higher temperatures, WAXD fiber patterns inserted in Fig. 3 show a smectic F (S_F) phase. A sharp low-angle reflection represents the layer spacing and a reflection at $2\theta=19^{\circ}$ is attributed to the lateral molecular packing into a hexagonal two-dimensional lattice. However, in this S_F phase, no long-range correlation of the structural order can be found between layers. Decreasing the temperature to below 130°C, the sample enters a new phase, the SC_G. In this phase, three-dimensional long-range structural order starts to form, and therefore correlation between layers becomes possible although the structure still fits into a hexagonal lattice. Upon decreasing the temperature to below 118°C, the crystal structure undergoes a sudden change from a hexagonal lattice to an orthorhombic lattice. This is the SC_H phase. As shown the inserted WAXD pattern, the reflections are completely different from the high temperature ones. This structure, with the highest order among these structures, remains until the glass transition temperate is reached.

Different structural orders in the samples must be associated with different molecular dynamics. As shown in Fig. 3 in TPP-15, there are three different phase structures before the isotropic melt is reached. Therefore, it can be expected that within these phases, molecular dynamics should also possess its own

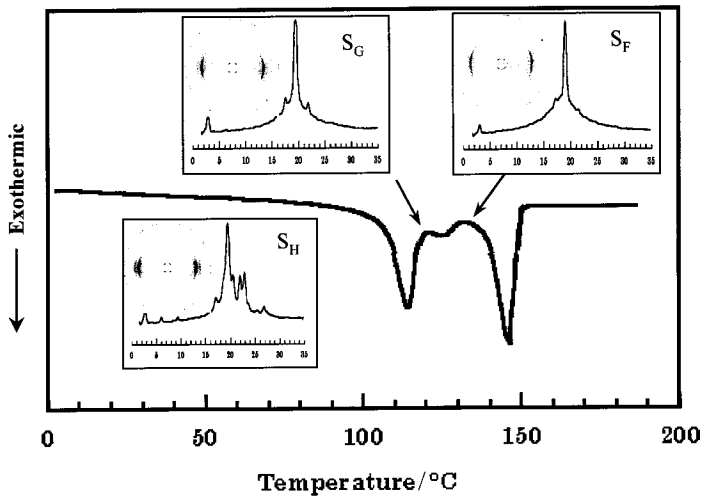

Fig. 3. A DSC cooling thermal diagram of TPP-15 from the isotropic melt. Multiple transition processes can be observed. The inserted WAXD patterns indicate the phase structures characterized within each phase.

characteristics. We have used temperature-controlled solid state C-13 NMR experiments to provide information of molecular dynamics of the polymer at different temperatures [61]. Our focus is on the dynamics of conformational changes of the methylene units in different phases using the y-gauche effect in the ^{13}CNMR chemical shift, which depends largely on the C–C conformation under the condition of magic angle spinning. The NMR results on the conformational order of the methylene units may be correlated with the entropy changes in the methylene units that are associated with phase transitions measured by DSC experiments. Both the entropy change of the methylene units and ^{13}CNMR chemical shift show that in the highly ordered smectic phase and smectic crystals of this polymer, the methylene units play an important role in maintaining the order of these phases. The correlation of the NMR results and DSC observations can be seen in Table 1. Note that in the DSC observations, the $\Delta S/\Delta S(I\leftrightarrow SC_H)$ is calculated based on the ratio of the entropy change of individual phase transition to the overall entropy change from the isotropic melt to the SC_H phase. Since the liquid crystalline transition is close to a thermodynamic equilibrium transition the entropy change can be easily calculated be the ratio of enthalpy change and transition temperature. On the other hand, the conformational order measured in NMR is calculated based on the ratio between the population of *trans*-conformation within each phase and overall change of the *trans*-conformation involved in these phase transitions. Indeed, both series of data fit very well, indicating the molecular dynamics are associated with the thermodynamic property changes in the phase transformations.

Table 1
Comparison of methylene unit contributions to the entropy changes and conformational order at liquid crystalline transitions in TPP-15 [61]

Transitions	$\Delta S/\Delta S(I\leftrightarrow SC_H)$	$\Delta\rho/\Delta\rho(I\leftrightarrow SC_H)$
$I\leftrightarrow S_F$	42%	46%
$S_F\leftrightarrow SC_G$	17%	17%
$SC_G\leftrightarrow SC_H$	42%	38%

4. Conclusions

In summary, thermal analysis techniques have been extensively developed during the past 40 years, and they will continue to play an important role in the research and development of materials science and technology as we are entering the next century. It is clear that thermal analysis techniques can be further improved by performing more precise measurements utilizing traditional techniques, and by combining in-situ temperature-controlled experiments for the study

of structures and dynamics, which are traditionally studied by diffraction, scattering, spectroscopy and microscopy. As another important part of this development, thermal analysis techniques should also be developed for use in quality control and on-line measurements during production. This has not been touched at all in this small commentary paper due to the lack of our experience in this area, but this is certainly not because this topic is any less important. On the contrary, we may expect that this application could bring and stimulate a broad inquiry of scientific knowledge and technical innovation.

Acknowledgements

This paper was supported by the NSF (DMR-96 17030).

References

[1] S.Z.D. Cheng, A. Keller, Ann. Rev. Mater. Sci. 28 (1998) 533.
[2] A. Keller, S.D.Z. Cheng, Polymer 39 (1998) 4461.
[3] S.Z.D. Cheng, L. Zhu, C.Y. Li, P.S. Honigfort, A. Keller, Thermochim. Acta 332 (1999) 105.
[4] B. Wunderlich, Thermal Analysis, Academic Press, New York, 1990.
[5] E.A. Turi (Ed.), Thermal Characterization on Polymeric Materials, 2nd Edition 1997, Academic Press, New York, 1981.
[6] V.B.F. Mathot, Calorimetry and Thermal Analysis on Polymers, Hanser, New York, 1993.
[7] W.W. Wendlandt, Thermal Analysis, 3rd Edition, Wiley, New York, 1985.
[8] B. Wunderlich, S.Z.D. Cheng, Gaz. Chem. Ital. 116 (1986) 345.
[9] B. Wunderlich, S. Z. D. Cheng, K. Loufakis, Thermodynamic Properties, Encyclopedia of Polymer Science and Engineering, 2nd Edition, Vol. 16, Wiley, New York, 1989, pp. 767–807.
[10] S.Z.D. Cheng, J Appl. Polym. Sci. Appl. Polym. Symp. 43 (1989) 315.
[11] M. J. Richardson, Thermal Analysis, in Comprehensive Polymer Science, Pergamon Press, New York, Vol. 1, 1988, (Chapter 36), pp. 867–898.
[12] B. Wunderlich, Macromolecular Physics, Crystal Structure, Morphology and Defects, Vol. 1, Academic Press, New York, 1973.
[13] B. Wunderlich, Macromolecular Physics, Crystal Nucleation, Growth, Annealing, Vol. 2, Academic Press, New York, 1976.
[14] B. Wunderlich, Macromolecular Physics, Crystal Melting, Vol. 3, Academic Press, New York, 1980.
[15] P. Geil, Polymer Single Crystals, Wiley/Interscience, New York, 1963.
[16] D.C. Bassett, Principles of Polymer Morphology, Cambridge University, New York, 1981.
[17] L. Mandelkern, Crystallization of Polymers, McGraw-Hill, New York, 1964.
[18] A. Keller, G. Goldbeck-Wood, in: A. Aggewal, Sir. J. Allen (Eds.), Comprehensive Polymer Science, Supplemental Two, Pergamon, Oxford, 1996, pp. 241–305.
[19] J.D. Hoffman, J.J. Weeks, J. Res. Natl. Bur. Stand. A 66 (1962) 13.
[20] H. Suzuki, J. Grebowicz, B. Wunderlich, Makromol. Chem. 189 (1985) 1109.
[21] H. Suzuki, J. Grebowicz, B. Wunderlich, Br. Polym. J. 17 (1985) 1.
[22] S.Z.D. Cheng, M.-Y. Cao, B. Wunderlich, Macromolecules 19 (1986) 1868.
[23] S.Z.D. Cheng, B. Wunderlich, Macromolecules 20 (1987) 1630.
[24] S.Z.D. Cheng, Z. Wu, B. Wunderlich, Macromolecules 20 (1987) 2802.
[25] S.Z.D. Cheng, B. Wunderlich, Macromolecules 21 (1988) 789.
[26] S.Z.D. Cheng, R. Pan, B. Wunderlich, Makromol. Chem. 189 (1988) 2243.
[27] S.Z.D. Cheng, D.P. Heberer, H.-S. Lien, F.W. Harris, J. Polym. Sci. Polym. Phys. Ed. 28 (1990) 655.
[28] S.-F. Lau, H. Suzuki, B. Wunderlich, J. Polym. Sci. Polym. Phys. Ed. 22 (1984) 379.
[29] J. Grebowicz, S.-F. Lau, B. Wunderlich, J. Polym. Sci. Polym. Symp. 71 (1984) 19.
[30] J. Menzel, B. Wunderlich, J. Polym. Sci. Polym. Lett. Ed. 19 (1981) 261.
[31] J.P. Arlie, P.A. Spegt, A.E. Skoulios, Makromol. Chem. 99 (1966) 170.
[32] J.P. Arlie, P.A. Spegt, A.F. Skoulios, Makromol. Chem. 104 (1967) 212.
[33] P.A. Spegt, Makromol. Chem. 139 (1970) 139.
[34] A.J. Kovacs, A. Gonthier, Colloid Polym. Sci. 250 (1972) 530.
[35] A.J. Kovacs, A. Gonthier, C. Straupe, J. Polym. Sci. Polym. Symp. 50 (1975) 283.
[36] A.J. Kovacs, C. Straupe, C.A. Gonthier, J. Polym. Sci. Polym. Symp. 59 (1977) 31.
[37] A.J. Kovacs, C. Straupe, J. Crystal Growth 48 (1980) 210.
[38] A.J. Kovacs, C. Straupe, Faraday Discuss. Chem. Soc. 68 (1979) 225.
[39] S.Z.D. Cheng, A.-Q. Zhang, J.-H. Chen, D.P. Heberer, J. Polym. Sci. Polym. Phys. Ed. 29 (1991) 287.
[40] S.Z.D. Cheng, J.-H. Chen, A.-Q. Zhang, D.P. Heberer, J. Polym. Sci. Polym. Phys. Ed. 29 (1991) 299.
[41] S.Z.D. Cheng, J.-H. Chen, J. Polym. Sd. Polym. Phys. Ed. 29 (1991) 311.
[42] S.Z.D. Cheng, A.-Q. Zhang, J.S. Barley, J.-H. Chen, A. Habensehuss, P.R. Zschack, Macromolecules 24 (1991) 3937.
[43] S.Z.D. Cheng, J.-H. Chen, A.-Q. Zhang, J.S. Barley, A. Habensehuss, P.R. Zschack, Polymer 33 (1992) 1140.

[44] S.Z.D. Cheng, J.-H. Chen, J.S. Barley, A.-Q. Zhang, A. Habensehuss, P.R. Zschack, Macromolecules 25 (1992) 1453.
[45] S.Z.D. Cheng, S.S. Wu, J.-H. Chen, Q. Zhuo, R.P. Quirk, E.D. von Meerwall, B.S. Hsiao, A. Habenschuss, P.R. Zschack, Macromolecules 26 (1993) 5105.
[46] S.-W. Lee, E. Chen, A.-Q. Zhang, Y. Yoon, B.S. Moon, S. Lee, F.W. Harris, E.D. von Meerwall, B.S. Hsiao, R. Verma, R.J.B. Lando, Macromolecules 29 (1996) 8816.
[47] E.-Q. Chen, S.-W. Lee, A.-Q. Zhang, B.S. Moon, S. Lee, F.W. Harris, S.Z.D. Cheng, B.S. Hsiao, F. Yei, Polymer 40 (1999) 4543.
[48] E.-Q. Chen, S.-W. Lee, A. Zhang, B.S. Moon, S. Lee, F.W. Harris, S.Z.D. Cheng, B.S. Hsiao, F. Yei, in ACS series, Scattering from Polymers, Vol. 739, Chapt. 8, pp. 118–139, 1999.
[49] E.-Q. Chen, S.-W. Lee, A.-Q. Zhang, B.S. Moon, S. Lee, F.W. Harris, S.Z.D. Cheng, B.S. Hsiao, F. Yei, Macromolecules 32 (1999) 4784.
[50] K. Song, S. Krimm, Macromolecules 23 (1990) 1946.
[51] I. Kim, S. Krimm, Macromolecules 29 (1996) 7186.
[52] G. Ungar, A. Keller, Polymer 27 (1986) 1835.
[53] G. Ungar, A. Keller, Polymer 28 (1987) 1899.
[54] D.G. Gray, Polymeric Liquid Crystals, A. Blumstein (Ed.), Plenum Press, New York, 1985.
[55] P.S. Pershan, Structure of Liquid Crystal Phases, World Scientific Publishing, Singapore, 1988.
[56] S.Z.D. Cheng, Y. Yoon, A.-Q. Zhang, E.P. Savitski, J.-Y. Park, V. Percec, P. Chu, Macromol. Rapid Commun. 16 (1995) 533.
[57] Y. Yoon, A.-Q. Zhang, R.-M. Ho, B. Moon, S.Z.D. Cheng, V. Percec, P. Chu, Macromolecules 29 (1996) 294.
[58] Y. Yoon, R.-M. Ho, B. Moon, D. Kim, K.W. Mccreight, F. Li, F.W. Harris, S.Z.D. Cheng, V. Percec, P. Chu, Macromolecules 29 (1996) 3421.
[59] R.-M. Ho, Y. Yoon, M. Leland, S.Z.D. Cheng, D. Yang, V. Percec, P. Chu, Macromolecules 29 (1996) 4528.
[60] R.-M. Ho, Y. Yoon, M. Lelend, S.Z.D. Cheng, V. Percec, P. Chu, Macromolecules 30 (1997) 3349.
[61] J. Cheng, Y. Yoon, R.-M. Ho, M. Leland, M. Guo, S.Z.D. Cheng, V. Percec, P. Chu, Macromolecules 30 (1997) 4688.
[62] R.-Q. Zheng, E.-Q. Chen, S.D. Cheng, F. Xie, D. Yan, T. He, V. Percec, P. Chu, G. Ungar, Macromolecules 32 (1999) 3574.